Integration Grid Errors for Meta-GGA-Predicted Reaction Energies: Origin of Grid Errors for the M06 Suite of Functionals

Steven E. Wheeler[*] and **K. N. Houk**
Department of Chemistry and Biochemistry, University of California, Los Angeles, CA 90095

Abstract

We have assessed integration grid errors arising from the use of popular DFT quadrature schemes for a set of 34 organic reaction energies. The focus is primarily on M05-2X and the M06 suite of functionals (M06-L, M06, M06-2X, and M06-HF). M05-2X, M06, and M06-2X outperform popular older DFT functionals for the reaction energies studied, and offer accuracies comparable to results from perturbative hybrid DFT functionals. However, these new functionals are more sensitive to the choice of quadrature grid than previous generations of DFT functionals. Errors in predicted reaction energies arising from the use of the popular SG-1 grid, which is the default in the Q-Chem package, are significant. In particular, M06-HF reaction energies computed with the SG-1 grid exhibit errors ranging from -6.7 to 3.2 kcal mol^{-1} relative to results computed with a very fine integration grid. This grid-sensitivity is not a problem for meta-GGA functionals in general, but is instead due to the specific functional forms used in these functionals. The large grid errors are traced to the kinetic energy density enhancement factor utilized in the exchange component of the M05-2X and M06 functionals. This term contains empirically adjusted parameters that are of large magnitude for all of the M06 functionals and for M06-HF in particular. The product of these large constants with modest integration errors for the kinetic energy density results in very large errors in individual contributions to the exchange energy. This gives rise to the troubling large errors exhibited by these functionals for certain integration grids.

I. Introduction

Kohn-Sham density functional theory (DFT) has emerged as the preeminent choice for the computational study of organic reactions. The popularity of DFT over traditional *ab initio* methods in this context stems from a number of factors, including favorable scaling with system size combined with relatively high-accuracy, widespread availability of analytic first and second energy derivatives for efficient geometry optimizations and vibrational frequency computations, and efficient implementations in popular electronic structure theory packages. Because the necessary integrals over exchange-correlation functionals cannot be evaluated in closed form, Kohn-Sham DFT computations typically rely on numerical quadrature schemes. In most quantum chemistry programs, these integrals are approximated as a sum of contributions from atom-centered grids,

$$\int F\left(\mathbf{r}\right) d\mathbf{r} \approx \sum_A^{atoms} \sum_g^{grid} w_g \, p_A\left(\mathbf{r}_g\right) F\left(\mathbf{r}_g\right)$$

(1)

swheele2@chem.ucla.edu.

where w_g are the quadrature weights at the corresponding grid points $\mathbf{r}_g$, and the atomic partitioning function, $p_A(\mathbf{r}_g)$, is defined such that $\sum_{A}^{atoms} p_A(\mathbf{r}_g) = 1$ at each point in space.

Various quadrature methods and atomic partitioning functions have been devised, several of which enjoy widespread use.[1-5] It has long been known (though not always appreciated!) that the choice of integration grid can significantly affect computed molecular properties.[6-9] Martin, Bauschlicher, and Ricca[6] studied the grid-sensitivity of B3LYP-computed molecular properties and highlighted problems with popular grids for several third-row transition metal systems and simple hydrocarbon radicals. More recently, Papas and Schaefer[7] compared BLYP and B3LYP energies from the Gaussian, Molpro, NWchem, Q-Chem, and GAMESS packages using default and finer integration grids to assess the precision that can be expected from the integration schemes in these packages. Dressler and Thiel[8] analyzed the effect of integration grids on DFT-computed anharmonic force fields, and Termath and Sauer[9] examined their effect on DFT-based direct molecular dynamics simulations.

Some recently developed DFT functionals that explicitly depend on the kinetic energy density (meta-GGAs) offer some significant advantages over previous generations of functionals.[10, 11] A shortcoming of these functionals that is often neglected, however, is the increased sensitivity to the choice of integration grid. By default, popular electronic structure programs utilize quadrature grids that were developed and refined based on previous generations of DFT functionals. Unfortunately, some integration grids that proved adequate for these older functionals can lead to significant errors when utilized with new meta-GGAs.[12-17]

In 2004, Johnson *et al.*[12] demonstrated that potential energy curves for dispersion-bound complexes computed with VS98[18] and other meta-GGA functionals are prone to spurious oscillations unless very large integration grids are used. Gräfenstein and Cremer subsequently proposed[17] the use of locally augmented radial integration grids to combat these issues in a cost-effective way. In 2009, Johnson and co-workers[13] revisited these grid errors and showed that the grid sensitivity originates from singularities near the intermonomer midpoint in kinetic energy density-dependent functional forms present in many meta-GGAs. Similarly, Gräfenstein, Izotov, and Cremer[14] attributed irregularities in certain meta-GGA energies for stretched covalent bonds to singularities in the self-interaction correction term present in the correlation part of these functionals.

The oscillations in meta-GGA-computed interaction potentials for dispersion-bound complexes[12] was addressed in the design of the M06 suite of functionals through the elimination of problematic terms in the VS98 functional, on which the M06 functionals are in part based.[10] The resulting changes in the M06 functionals offer improved performance in this regard, although with some popular grids problems still arise.[13,15,16] For example, Merz and co-workers[15] recently analyzed the performance of a number of methods for the prediction of potential energy curves for model non-covalent interactions. The M06-2X and M06-L DFT functionals outperformed the other methods tested, but yielded discontinuous energy curves when used with the popular SG-1 integration grid.[16]

Grid issues with these meta-GGA functionals are not limited to dispersion-bound complexes. For example, Csonka and co-workers[19] benchmarked a variety of DFT functionals for the prediction of geometries and conformational energies of a series of saccharides. Although M05-2X yielded the most reliable results of the tested methods when a dense integration grid was used, results computed using the default integration grid in the Jaguar program package lead to larger errors in energies and problems in geometry optimizations. Similarly, Scuseria and co-workers[20] recently reported geometry optimization convergence problems and spurious imaginary frequencies when pairing functionals from the M06 suite with various popular integration grids.

In the present work we focus on the grid requirements for meta-GGA-predicted energies for a set of 34 organic isomerization reactions recently published by Grimme and co-workers.[21] This set, shown in Scheme 1, constitutes a diverse collection of reactions that are small enough for the application of accurate benchmark computations yet representative of the diverse changes in bonding that occur in organic reactions. Reference "experimental reaction energies" were derived from standard enthalpies of formation corrected for zero-point vibrational and thermal effects by Grimme.[21] All of the reactions are endothermic as written. Our primary focus is on grid errors for M05-2X and the M06 family of functionals,[10] which have emerged as promising new functionals for diverse chemical applications.[22]

II. Theoretical Methods

Single point energies were computed for the molecular species in Scheme 1 using five meta-GGA DFT functionals paired with various DFT integration grids. The TZV(2df,2pd) basis set[23,24] was used for all computations, which were executed at B3LYP/TZV(p,d) optimized geometries taken from [Ref 21]. The TZV(2df,2pd) basis set comprises the Alrichs TZV triple-ζ quality basis set[23] plus polarization functions from the cc-pVTZ basis set.[24] Grid errors for other popular basis sets are expected to be similar. The meta-GGAs tested are VS98,[18] M05-2X, [25] M06-L,[26] M06-HF,[27] M06,[10] and M06-2X.[10] For comparison, grid errors for B3LYP,[28] PBE,[29,30] and TPSS[31] are also presented.

The atom-centered grids utilized in popular DFT codes are constructed as a direct product of sets of N^r radial and N^Ω angular grid points,

$$\sum_g^{grid} w_g F\left(\mathbf{r}_g\right) = \sum_{i=1}^{N^r} w_i^r \sum_{i=1}^{N^\Omega} w_j^\Omega F\left(\mathbf{r}_i, \theta_j, \varphi_j\right)$$

(2)

Defining an integration grid requires a choice of atomic partitioning function and the number, weights, and distribution of radial and angular grid points.

Four popular integration grids were tested (see Table 1). Grids labeled "Q-Chem", "NWChem", and "Gaussian" are equivalent to the default grids in those packages.[32-35] The default Q-Chem grid is the popular SG-1 grid of Gill, Johnson, and Pople.[16] All of the tested grids rely on Lebedev's angular quadrature.[1] The radial components of these grids are from either an Euler-Maclaurin quadrature with the coordinate transformation of Murray, Handy, and Laming (Euler)[2] or the modification of the Murray-Handy-Laming scheme published by Mura and Knowles (MK).[3] For the atomic partitioning functions, the tested grids use the scheme of Becke,[5] the modification introduced by Stratmann, Scuseria, and Frisch (SSF),[4] or an unpublished modification of the SSF scheme (Erf1) implemented in NWChem[33,34] in which the partition function weights are written in terms of products of error functions.

Most program packages utilize automatically pruned integration grids, in which the number of angular points is dependent on the radial coordinate.[16] This leads to significant reductions in computational cost with minimal loss in accuracy compared to the use of the unpruned grid. The effect of pruning was tested for selected reaction energies. Errors arising from pruning were less than 0.1 kcal mol^{-1} across all grids considered and are considered inconsequential. Presented results are based on pruned grids.

Energies computed using the NWChem "Xfine" grid (see Table 1) were used as a benchmark [i.e.: $\Delta E_{grid}^{error} = \Delta E_{grid} - \Delta E_{XFine}$]. To confirm that reaction energies computed using this grid are converged with respect to integration grid density, the M06-2X reaction energies, which are

the most sensitive to the choice of grid, were also computed using a grid with 300 radial points and 1202 angular points. The mean absolute deviation in reaction energies between the Xfine grid and this very large integration grid was only 0.0003 kcal mol^{-1}; the maximum deviation is 0.003 kcal mol^{-1}. With these meta-GGA functionals, use of default convergence criteria sometimes lead to convergence problems and resulted in erratic and seemingly irreproducible grid errors. This was particularly true for the less dense grids and the M06-HF functional. Care was taken to ensure that all energies are converged to the correct Kohn-Sham solution to a precision of at least 10^{-10} *au*. Converging DFT energies to this precision is often hampered by screening thresholds for integrals and the electron density employed by popular DFT programs. In this work, screening thresholds of at least 10^{-14} *au* were used.[36] Much larger errors than reported here could be encountered with these functionals if care is not taken to tightly converge results.

All computations were carried out using a locally modified version of NWChem 5.1.[33,34]

III. Results and Discussion

The present work is primarily concerned with grid errors in computed reaction energies, not the error in the reaction energies themselves or the grid errors in absolute energies. However, since the accuracy of most of the tested functionals has not been previously assessed for the reactions in Scheme 1, a brief analysis of the reaction energy errors compared to experiment is presented first. This allows the subsequent analysis of grid errors to be put into the perspective of the inherent error in the DFT computations.

A. Performance of meta-GGA Functionals for Reaction Energies

Errors in DFT-computed reaction energies, relative to experimental results,[21] are shown in Table 2. These values were computed using the XFine integration grid. Mean signed deviations, mean absolute deviations, and the range of deviations from experiment are plotted in Fig. 1. Of the functionals tested here, the M05-2X, M06, and M06-2X functionals offer the best performance, although even these functionals exhibit errors approaching ±5 kcal mol^{-1} for selected reactions. The mean deviations for the M05-2X, M06, and M06-2X functionals are comparable to those from mPW2-PLYP,[37] B2-PLYP,[38] and BMK[39] for this test set.[21] The B3LYP, PBE, TPSS, M06-L, and M06-HF functionals perform less well and are all comparable. VS98 performs more poorly for these reactions, delivering the largest mean error and a very large error for reaction (11).

B. Errors with Popular Integration Grids

Integration grid errors have been assessed for the 34 organic isomerizations in Scheme 1. The grid errors for four popular quadrature grids are summarized in Table 3. Details for each reaction are provided in Supporting Information (SI). Normalized error distributions for the B3LYP, PBE, and TPSS functionals are shown in Fig. 2. Analogous plots for VS98, M05-2X, and the four M06 functionals are shown in Fig. 3. For B3LYP, PBE and TPSS, grid errors arising from the use of the NWChem, Gaussian, and Fine grids are negligible, never exceeding ±0.1 kcal mol^{-1}. The errors are slightly larger for the Q-Chem grid, and there is one outlier [reaction (11)] at 0.7 kcal mol^{-1}, 0.8 kcal mol^{-1}, and 0.8 kcal mol^{-1} for B3LYP, PBE, and TPSS, respectively. Overall, the grid requirements for these three functionals are modest and the errors resulting from any of these grids are far less than the errors in the computed reaction energies (compare Tables 2 and 3).

For VS98, M05-2X, and the four M06 functionals (Fig. 3), the grid errors are significantly larger than for B3LYP, PBE, or TPSS. Even so, the errors arising from the use of the Gaussian and Fine integration grids are tightly grouped around zero and never exceed 0.15 kcal mol^{-1}

for M05-2X or the M06 suite of functionals. For the NWChem grid, the errors are only slightly larger than the Gaussian and Fine grid results, although the magnitude exceeds 0.5 kcal mol^{-1} in several cases. The most troubling results arise from use of the Q-Chem (SG-1) grid,[16] which leads to significant errors in computed reaction energies. The problems are most severe for the M06-HF functional, for which the grid errors range from −6.7 to 3.2 kcal mol^{-1}. For M06-HF computations employing this popular grid, these grid errors will be the dominant source of error and predicted reaction energies will generally be qualitatively different than those computed with finer integration grids.

Across all of these functionals, the largest grid errors occur for reaction (10) followed by (11). However, not all functionals behave uniformly. For example, with the Q-Chem grid, the M06-HF predicted energy for reaction (11) is within 1.7 kcal mol^{-1} of the Xfine reference, while the energy for reaction (10) deviates by 5.6 kcal mol^{-1}. For the M05-2X functional, the energy for reaction (11) falls 0.4 kcal mol^{-1} from the reference value, even though the value for reaction (10) is in error by only −0.1 kcal mol^{-1}. This non-systematic behavior is indicative of an underlying cancelation of more sizeable errors, which is discussed in detail below. Reaction (10) has been highlighted previously[16] as a case prone to grid errors. Gill and co-workers[16] attributed this to the large difference in shape of the two isomers of pentane. Essentially, for more "compact" molecules (*e.g.*: neopentane), the same number of grid points covers a smaller amount of space, so the grid error in the absolute energy should be reduced compared to the error for less compact species (*e.g.*: *n*-pentane).

C. Effects of Atomic Partitioning Function and Radial Quadrature Methods

To quantify the effect of different atomic partitioning functions and radial quadrature schemes, the errors associated with grids comprising 50 radial points and 194 angular points are examined more closely. Errors for six combinations of atomic partitioning function and radial quadrature scheme are summarized in Table 4. The leftmost column (Becke/Euler) is the Q-Chem (SG-1) grid.[16] Normalized error distributions for the six meta-GGAs paired with these six grids are shown in Fig. 4. The Euler and MK radial quadrature schemes[2,3] perform similarly, regardless of the partitioning function. The MK scheme provides a minimal reduction in mean grid errors compared to the Euler method. On the other hand, the choice of partitioning function has a significant impact on grid errors for all functionals considered. The SSF or Erf1 partitioning functions[4] result in significantly smaller mean errors compared to the Becke results.[5] These results are in accord with previous findings of Martin *et al.*[6] and the assertion by Scuseria and co-workers[4] that the SSF scheme[4] is numerically more stable than that of Becke.[5] However, for the M06-HF functional, none of these grids tested delivers reaction energies with errors consistently below 0.5 kcal mol^{-1}.

D. Origin of Grid Errors

In order to unravel the origins of the large grid errors arising from the use of the Q-Chem (SG-1) grid,[16] the contributions to these errors are examined in more detail. Normalized error distributions for the exchange (E_x) and correlation (E_c) components of the reaction energies are shown in Fig. 5.[40] Mean grid errors in E_x and E_c are given in SI Table S2. For all but the VS98 functional, the errors in E_x swamp those arising from E_c, for which the MADs are less than 0.1 kcal mol^{-1}. For the VS98 functional, the situation is reversed; in this case E_c exhibits a larger MAD than E_x. Regardless, the unsettling grid errors exhibited by M05-2X and the M06 functionals arise from the exchange energies.

The exchange functional utilized for the M06 suite[10] is a linear combination of the functional forms of the M05-2X[25] and VS98[18] exchange functionals,

$$E_x^{\text{M06}} = E_x^{\text{"M05-2X"}} + E_x^{\text{"VS98"}}.$$

<div style="text-align: right">(3)</div>

$E_x^{\text{"M05-2X"}}$ is the PBE exchange functional, $F_{x_\sigma}^{\text{PBE}}$, multiplied by a kinetic energy density-dependent term, $f(w_\sigma)$. This function is referred to by Truhlar and co-workers[10] as the "kinetic energy density enhancement factor", and is written as a power series in w_σ. w_σ in turn is a function of the spin kinetic energy density.[41] The form for the M06 exchange functional is given in Eq (4), where ρ_σ, $\nabla\rho_\sigma$, and τ_σ are the spin-density, gradient, and kinetic energy density, respectively, and d_i and a_i are empirically determined parameters. Setting a_0 to 1.0 and the other a_i and d_i constants to zero gives the standard PBE GGA exchange functional, while setting the a_i constants to zero (and the d_i to the appropriate values) yields VS98 exchange. The M05-2X exchange functional is obtained by setting the d_i constants to zero, and the a_i to the appropriate values.

$$E_x^{\text{M06}} = \sum_\sigma^{\alpha,\beta} \int d\mathbf{r} \left[F_{x_\sigma}^{\text{PBE}}(\rho_\sigma, \nabla\rho_\sigma) f(w_\sigma) + \varepsilon_{x_\sigma}^{\text{LSDA}} \left(\frac{d_0}{\gamma(x_\sigma, z_\sigma)} + \frac{d_1 x_\sigma^2 + d_2 z_\sigma}{\gamma^2(x_\sigma, z_\sigma)} + \frac{d_3 x_\sigma^4 + d_4 x_\sigma^2 z_\sigma + d_5 z_\sigma^2}{\gamma^3(x_\sigma, z_\sigma)} \right) \right]$$

<div style="text-align: right">(4)</div>

$$f(w_\sigma) = \sum_{i=0}^{11} a_i w_\sigma^i$$

<div style="text-align: right">(5)</div>

$$\varepsilon_{x_\sigma}^{\text{LSDA}} = \frac{3}{2} \left(\frac{3}{4\pi} \right)^{1/3} \rho_\sigma^{4/3}$$

<div style="text-align: right">(6)</div>

$$x_\sigma = \frac{|\nabla\rho_\sigma|}{\rho_\sigma^{4/3}}$$

<div style="text-align: right">(7)</div>

$$z_\sigma = \frac{2\tau_\sigma}{\rho^{5/3}} - \frac{3}{5}\left(6\pi^2\right)^{2/3}$$

<div style="text-align: right">(8)</div>

$$\gamma(x_\sigma, z_\sigma) = 1 + \alpha\left(x_\sigma^2 + z_\sigma\right)$$

<div style="text-align: right">(9)</div>

$$w_\sigma = (t_\sigma - 1)/(t_\sigma + 1)$$

<div style="text-align: right">(10)</div>

$$t_\sigma = \frac{3\left(6\pi^2\right)^{2/3} \rho_\sigma^{5/3}}{10\tau_\sigma}$$

(11)

Errors arising from the use of the Q-Chem grid for each term in Eq (4) are summarized in SI Tables S2 and S3. These were computed using converged densities from XFine computations with a locally modified version of NWChem 5.1.[33,34] Distributions of grid errors arising from the two main components of the M06-HF exchange functional, $E_x^{\text{"M05-2X"}}$ and $E_x^{\text{"VS98"}}$, are shown in Fig. 6a. The grid errors arise primarily from the M05-2X component.

Normalized grid error distributions for each power of w_σ in $f(w_\sigma)$ are plotted in Fig. 6b with all of the a_i constants set to unity [*i.e.*: $\sum_\sigma^{\alpha,\beta} \int d\mathbf{r} F_{X\sigma}^{PBE}(\rho_\sigma, \nabla\rho_\sigma) w_\sigma^i$]. The grid errors for each term are modest and exceed 0.5 kcal mol^{-1} for only a few reactions. The tendency is for the magnitude of the integration error to gradually increase with the power of w_σ, although for some reactions the integration errors are negligible for all powers of w_σ (errors for representative reactions are shown in Fig. 6c). The empirical constants a_i, on the other hand, vary considerably in magnitude and oscillate between negative and positive values (see Table 5). The grid errors for each term in $E_x^{\text{"M05-2X"}}$ will be the product of the a_i constant with the integration error for the corresponding power of w_σ. Because the magnitudes of the a_i constants are large, grid errors for the individual contributions to $f(w_\sigma)$ are enormous. For example, for reaction (10) the errors in the w_σ^7 and w_σ^9 terms are +82 and −132 kcal mol^{-1}, respectively. These sizeable errors mostly cancel due to the almost monotonic change in grid errors with each power of w_σ (see Fig. 6c) combined with the oscillations in the a_i constants. This cancelation is incomplete, of course, and gives rise to the troubling spread of grid errors discussed above. The substantial grid errors exhibited by the M06-HF functional in particular are a result of the very large a_i constants defining that functional (in particular, see the a_7 and a_9 constants for M06-HF in Table 5).

The attribution of these errors to the particular functional form used in the M06 suite of functionals is further supported by the qualitatively different grid-dependence exhibited by the meta-GGA functional TPSS. This functional, which does not contain a polynomial expansion in terms of the kinetic energy density, exhibits very modest dependence on the choice of integration grid; TPSS grid errors are on par with those from popular GGAs.

These grid errors are qualitatively different from those underlying the discontinuities in meta-GGA-computed potential energy curves for dispersion-bound complexes,[12] which arise from singularities in the τ-dependent functional forms.[13] The grid errors in reaction energies arise from modest errors in the integration of w_σ amplified by the large empirical a_i constants. One consequence is that these errors vary smoothly across potential energy surfaces. This is demonstrated for neopentane in SI Figs. S1 and S2, in which grid errors in the M06-HF energy computed with the Q-Chem grid are plotted as a function of the C–C and C–H bond lengths.

IV. Summary and Conclusions

DFT is invaluable in the computational study of organic reactions, and can provide accurate energies for large molecular systems that are beyond the reach of traditional *ab initio* methods. New DFT functionals offer increased accuracy and broader applicability compared to previous generations of functionals and have enabled the application of DFT to myriad new problems in organic chemistry and molecular biology. However, these new functionals are not without

drawbacks, one of which is the increased sensitivity of energies and other properties to the choice of integration grid. Previously documented[12-16] grid-sensitivities exhibited by these functionals include the prediction of potential energy curves for dispersion-bound complexes with spurious oscillations, as well problems with predicted energies, geometries, and vibrational frequencies.[19,20] We have quantified integration grid errors for six meta-GGA functionals (VS98, M05-2X, M06-L, M06, M06-2X, and M06-HF) paired with popular integration grids for 34 organic isomerization energies. The popular SG-1 grid,[16] which is the default in the Q-Chem package, leads to large errors for all of these functionals, and very large errors for M06-HF. This grid should not be used with any of these functionals. By contrast, the grid errors in B3LYP, PBE, and TPSS computed energies are small for all of the grids tested. Use of the SSF[4] or Erf1 atomic partitioning functions reduces grid errors compared to the standard SG-1 grid,[16] which utilizes the partitioning function of Becke.[5] However, the M06-HF functional still exhibits grid errors exceeding 0.5 kcal mol^{-1} for several of the reactions.

The grid errors exhibited by the M06 suite of functionals arise from integration errors in the exchange component of the energy. In particular, the significant errors arising from the use of the Q-Chem (SG-1) grid are due to the large empirical constants in the kinetic energy density enhancement factor. Some of these constants are of considerable size, and amplify modest errors in the integration of the kinetic energy density. This is not a general weakness of meta-GGAs, but a problem arising from the particular functional form used in the M06 suite of functionals.

Zhao and Truhlar recently published[11] the M08-HX and M08-SO functionals, which incorporate more flexible functional forms than members of the M06 suite and contain an altered self-interaction correction term that avoids the numerical instabilities discussed by Gräfenstein, Izotov, and Cremer.[14] Although the grid errors associated with these new functionals were not tested here, the kinetic energy density enhancement factor in M08-HX and M08-SO is the same as in the M06 functionals. Moreover, the empirical coefficients in this factor are larger than in any of the M06 suite of functionals, so M08-HX and M08-SO grid errors computed with the SG-1 grid are expected to be even more severe than observed for M06-HF.

The popularity of DFT and ease with which many computational chemistry program packages can be used has lead to a continued increase in the application of DFT to chemical problems by non-specialists. While this is certainly a welcome development and a testament to the maturity of the field of Kohn-Sham DFT, the present results offer a poignant reminder of the dangers of employing "default" options in any program package. These defaults are not suitable for all applications, and in the case of DFT integration grids the defaults in some cases are woefully inadequate for some meta-GGA functionals. In particular, use of the SG-1 integration grid with M05-2X or the M06 suit of functionals can result in significant errors in predicted reaction energies.

Supplementary Material

Refer to Web version on PubMed Central for supplementary material.

Acknowledgments

References

1. Lebedev VI, Laikov DN. Dokl Math 1999;59:477.

2. Murray CW, Handy NC, Laming GL. Mol Phys 1993;78:997.

3. Mura ME, Knowledge PJ. J Chem Phys 1996;104:9848.

4. Stratmann RE, Scuseria GE, Frisch MJ. Chem Phys Lett 1996;257:213.

5. Becke A. J Chem Phys 1988;88:1053.

6. Martin JML, Bauschlicher CW Jr, Ricca A. Computer Phys Comm 2001;133:189.

7. Papas BN, Schaefer HF. J Mol Struct THEOCHEM 2006;768:175.

8. Dressler S, Thiel W. Chem Phys Lett 1997;273:71.

9. Termath V, Sauer J. Chem Phys Lett 1996;255:187.

10. Zhao Y, Truhlar DG. Theo Chem Acc 2008;120:215.

11. Zhao Y, Truhlar DG. J Chem Theory Comput 2008;4:1849.

12. Johnson ER, Wolkow RA, DiLabio GA. Chem Phys Lett 2004;394:334.

13. Johnson ER, Becke A, Sherrill CD, DiLabio GA. J Chem Phys 2009;131:034111. [PubMed: 19624185]

14. Gräfenstein J, Izotov D, Cremer D. J Chem Phys 2007;127:214103. [PubMed: 18067345]

15. Fusti-Molnar L, He X, Wang B, Merz KM Jr. J Chem Phys 2009;131:065102. [PubMed: 19691412]

16. Gill PMW, Johnson BG, Pople JA. Chem Phys Lett 1993;209:506.

17. Gräfenstein J, Cremer D. J Chem Phys 2007;127:164113. [PubMed: 17979325]

18. Van Voorhis T, Scuseria G. J Chem Phys 1998;109:400.

19. Csonka GI, French AD, Johnson GP, Stortz CA. J Chem Theory Comput 2009;5:679.

20. Jiménez-Hoyos CA, Janesko BG, Scuseria GE. Phys Chem Chem Phys 2008;10:6621. [PubMed: 18989473]

21. Grimme S, Steinmetz M, Korth M. J Org Chem 2007;72:2118. [PubMed: 17286442]

22. Zhao Y, Truhlar DG. Acc Chem Res 2008;41:157. [PubMed: 18186612]

23. Schafer A, Huber C, Ahlrichs R. J Chem Phys 1994;100:5829.

24. Dunning TH Jr. J Chem Phys 1989;90:1007.

25. Zhao Y, Schultz NE, Truhlar DG. J Chem Theory and Comp 2006;2:364.

26. Zhao Y, Truhlar DG. J Chem Phys 2006;125:194101. [PubMed: 17129083]

27. Zhao Y, Truhlar DG. J Phys Chem A 2006;110:13126. [PubMed: 17149824]

28. Becke AD. J Chem Phys 1993;98:5648.

29. Perdew JP, Burke K, Ernzerhof M. Phys Rev Lett 1996;77:3865. [PubMed: 10062328]

30. Perdew JP, Burke K, Ernzerhof M. Phys Rev Lett 1997;78:1396.

31. Tao J, Perdew JP, Staroverov V, Scuseria G. Phys Rev Lett 2003;91:146401. [PubMed: 14611541]

32. Shao Y, Fusti-Molnar L, Jung Y, Kussmann J, Ochsenfeld C, Brown ST, Gilbert ATB, Slipchenko LV, Levchenko SV, O' Neill DP Jr, D RA, Lochan RC, Wang T, Beran GJO, Besley NA, H JM, Lin CY, Voorhis TV, Chien SH, Sodt A, Steele RP, Rassolov VA, Maslen PE, Korambath PP, Adamson RD, Austin B, Baker J, Byrd EFC, Dachsel H, Doerksen RJ, Dreuw A, Dunietz BD, Dutoi AD, Furlani TR, Gwaltney SR, Heyden A, Hirata S, Hsu CP, Kedziora G, Khalliulin RZ, Klunzinger P, Lee AM, Lee MS, Liang W, Lotan I, Nair N, Peters B, Proynov EI, Pieniazek PA, Rhee YM, Ritchie J, Rosta E, Sherrill CD, Simmonett AC, Subotnik JE, Woodcock HL III, Zhang W, Bell AT, Chakraborty AK, Chipman DM, Keil FJ, Warshel A, Hehre WJ, Schaefer HF, Kong J, Krylov AI, Gill PMW, Head-Gordon M. Phys Chem Chem Phys 2006;8:3172. [PubMed: 16902710]

33. Kendall RA, Apra E, Bernholdt DE, Bylaska EJ, Dupuis M, Fann GI, Harrison RJ, Ju J, Nichols JA, Nieplocha J, Straatsma TP, Windus TL, Wong AT. Computer Phys Comm 2000;128:260.

34. Bylaska, EJ.; de Jong, WA.; Govind, N.; Kowalski, K.; Straatsma, TP.; Valiev, M.; Wang, D.; Aprà, E.; Windus, TL.; Hammond, J.; Nichols, P.; Hirata, S.; Hackler, MT.; Zhao, Y.; Fan, PD.; Harrison, RJ.; Dupuis, M.; Smith, DMA.; Nieplocha, J.; Tipparaju, V.; Krishnan, M.; Wu, Q.; Van Voorhis, T.; Auer, AA.; Nooijen, M.; Brown, E.; Cisneros, G.; Fann, GI.; Fruchtl, H.; Garza, J.; Hirao, K.; Kendall, R.; Nichols, JA.; Tsemekhman, K.; Wolinski, K.; Anchell, J.; Bernholdt, D.; Borowski, P.;

Clark, T.; Clerc, D.; Dachsel, H.; Deegan, M.; Dyall, K.; Elwood, D.; Glendening, E.; Gutowski, M.; Hess, A.; Jaffe, J.; Johnson, B.; Ju, J.; Kobayashi, R.; Kutteh, R.; Lin, Z.; Littlefield, R.; Long, X.; Meng, B.; Nakajima, T.; Niu, S.; Pollack, L.; Rosing, M.; Sandrone, G.; Stave, M.; Taylor, H.; Thomas, G.; van Lenthe, J.; Wong, A.; Zhang, Z. NWChem, A Computational Chemistry Package for Parallel Computers, Version 5.1. Pacific Northwest National Laboratory; Richland, Washington 99352-0999, USA: 2007.

35. Frisch, MJ.; Trucks, GW.; Schlegel, HB.; Scuseria, GE.; Robb, MA.; Cheeseman, JR.; Montgomery, JA., Jr; Vreven, T.; Kudin, KN.; Burant, JC.; Millam, JM.; Iyengar, SS.; Tomasi, J.; Barone, V.; Mennucci, B.; Cossi, M.; Scalmani, G.; Rega, N.; Petersson, GA.; Nakatsuji, H.; Hada, M.; Ehara, M.; Toyota, K.; Fukuda, R.; Hasegawa, J.; Ishida, M.; Nakajima, T.; Honda, Y.; Kitao, O.; Nakai, H.; Klene, M.; Li, X.; Knox, JE.; Hratchian, HP.; Cross, JB.; Bakken, V.; Adamo, C.; Jaramillo, J.; Gomperts, R.; Stratmann, RE.; Yazyev, O.; Austin, AJ.; Cammi, R.; Pomelli, C.; Ochterski, JW.; Ayala, PY.; Morokuma, K.; Voth, GA.; Salvador, P.; Dannenberg, JJ.; Zakrzewski, VG.; Dapprich, S.; Daniels, AD.; Strain, MC.; Farkas, O.; Malick, DK.; Rabuck, AD.; Raghavachari, K.; Foresman, JB.; Ortiz, JV.; Cui, Q.; Baboul, AG.; Clifford, S.; Cioslowski, J.; Stefanov, BB.; Liu, G.; Liashenko, A.; Piskorz, P.; Komaromi, I.; Martin, RL.; Fox, DJ.; Keith, T.; Al-Laham, MA.; Peng, CY.; Nanayakkara, A.; Challacombe, M.; Gill, PMW.; Johnson, B.; Chen, W.; Wong, MW.; Gonzalez, C.; Pople, JA. Gaussian 03, Revision C.02. Gaussian, Inc.; Wallingford CT: 2004.

36. Note that as implemented in NWChem 5.1.1, the density screening threshold used by other functionals is overridden by the VS98, M05-2X, and M06 suite of functionals. Instead, in NWChem 5.1.1, density screenings for the exchange component of these functionals are fixed at 10^{-7} or 10^{-8} au.

37. Grimme S, Schwabe T. Phys Chem Chem Phys 2006;8:4398. [PubMed: 17001405]

38. Grimme S. J Chem Phys 2006;124:034108. [PubMed: 16438568]

39. Boese AD, Martin JML. J Chem Phys 2004;121:3405. [PubMed: 15303903]

40. The decomposition of grid errors for DFT energies into exchange and correlation components is complicated by the secondary effects of the grid errors on the SCF procedure. Even though the other components of the electronic energy (Coulomb and one-electron terms and HF exchange) are evaluated analytically and should exhibit no grid errors, when the Kohn-Sham orbitals are optimized, grid the errors in E_x and E_c lead to differences in all of the components of the energy for different grids. As such, to evaluate the errors arising from Ec and Ex, energies for the Q-Chem grid were evaluated using converged Kohn-Sham orbitals from Xfine grid computations. This has only a minor effect on the grid errors in the total reaction energies.

41. Becke A. J Chem Phys 2000;112:4020.
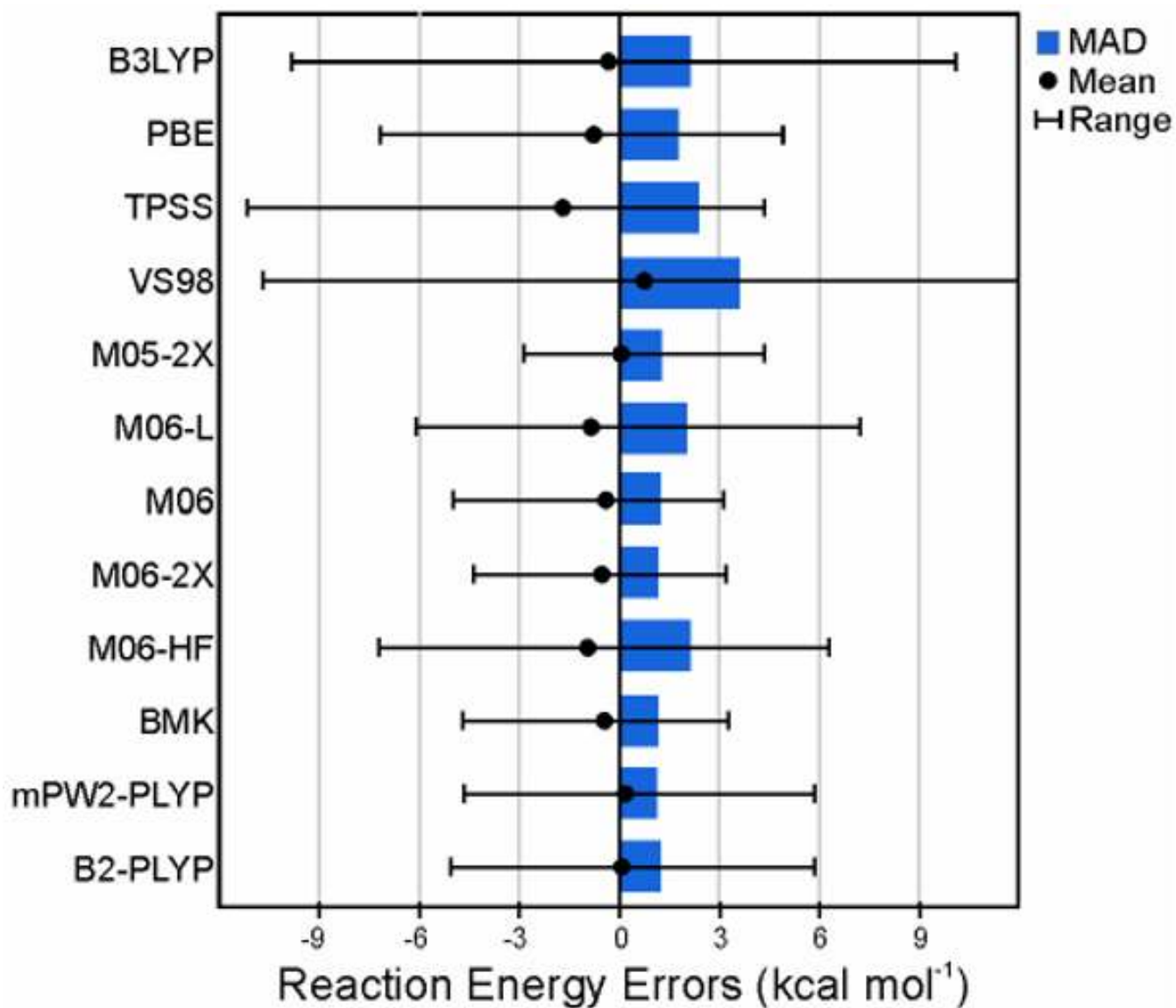
Figure 1.
Mean absolute deviations (MAD), mean signed deviations (MSD), and range of deviations from experiment for computed energies of the reactions in Scheme 1 (kcal mol^{-1}).
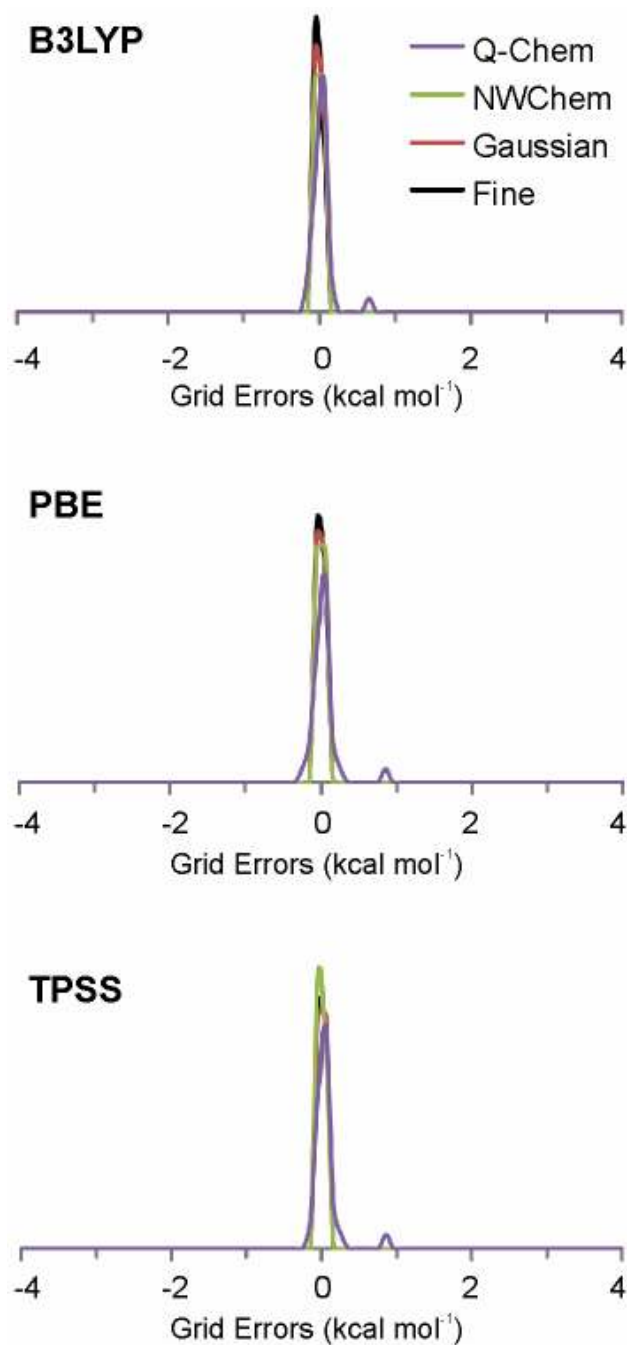
Figure 2.
Normalized distributions of grid errors (kcal mol^{-1}) for the energies of the reactions in Scheme 1, computed using four popular quadrature grids paired with the B3LYP, PBE, and TPSS functionals. Grids labeled "Q-Chem", "NWChem", and "Gaussian" are equivalent to the default grids in those packages. All computations were carried out using the NWChem program.[33,34]
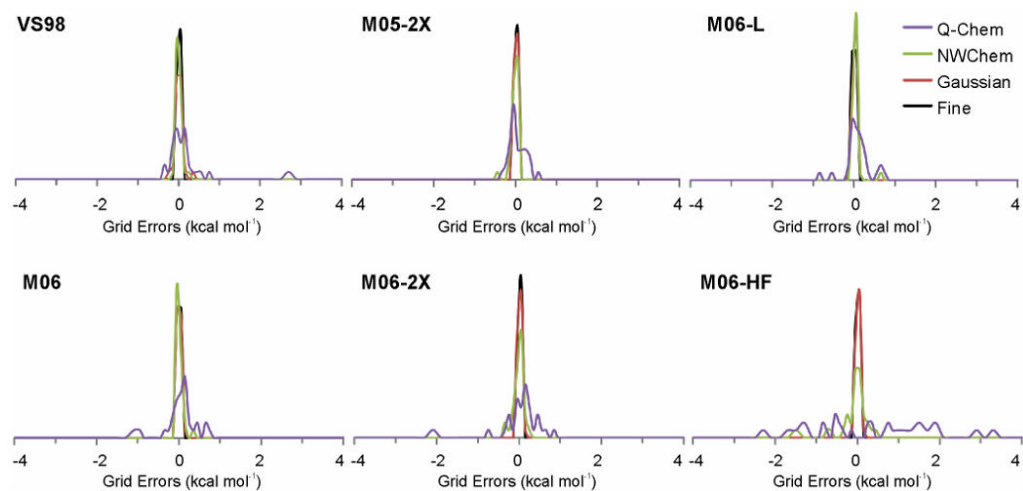
Figure 3.
Normalized distributions of grid errors (kcal mol^{-1}) for the energies of the reactions in Scheme 1 using four popular quadrature grids.
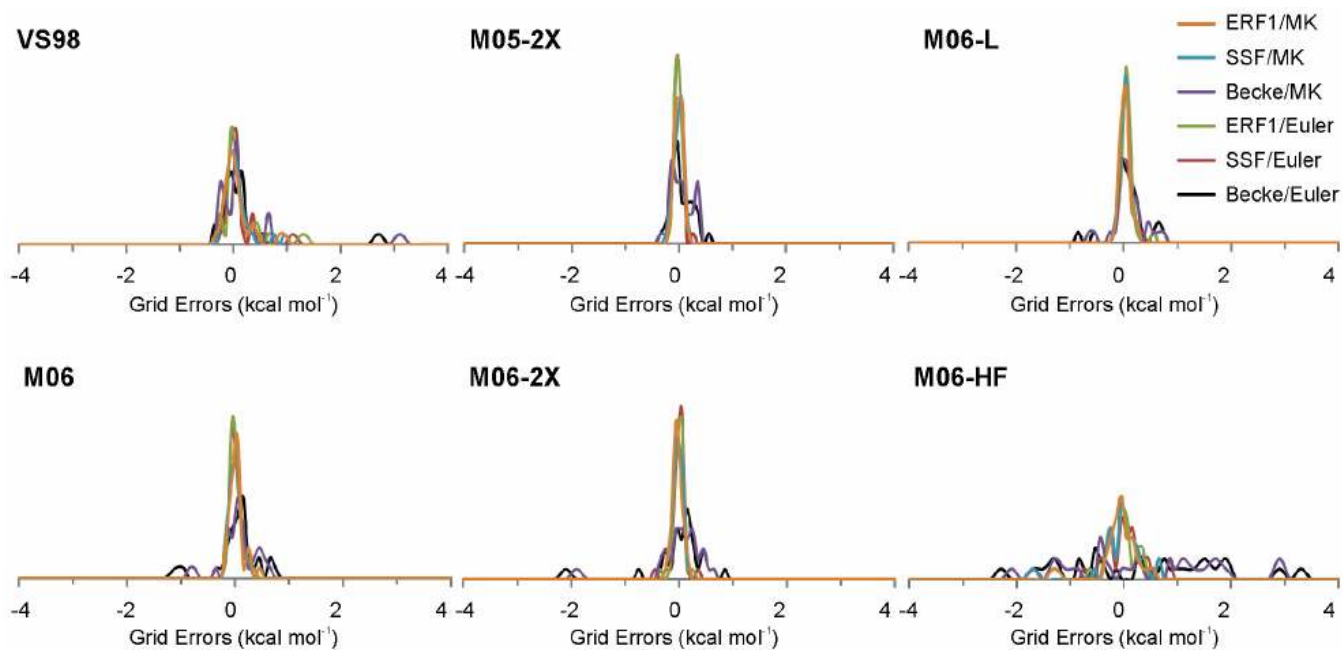
Figure 4.
Normalized distributions of grid errors (kcal mol^{-1}) for the energies of the reactions in Scheme 1 using six combinations of partitioning functions (Becke,[5] SSF,[4] or Erf1) and radial quadrature schemes [Euler-Maclaurin (Euler)[2] or Mura-Knowles (MK)[3]]. All grids are pruned and have 50 radial points and 194 angular points. The Becke/Euler combination corresponds to the default Q-Chem (SG-1) grid.[16]
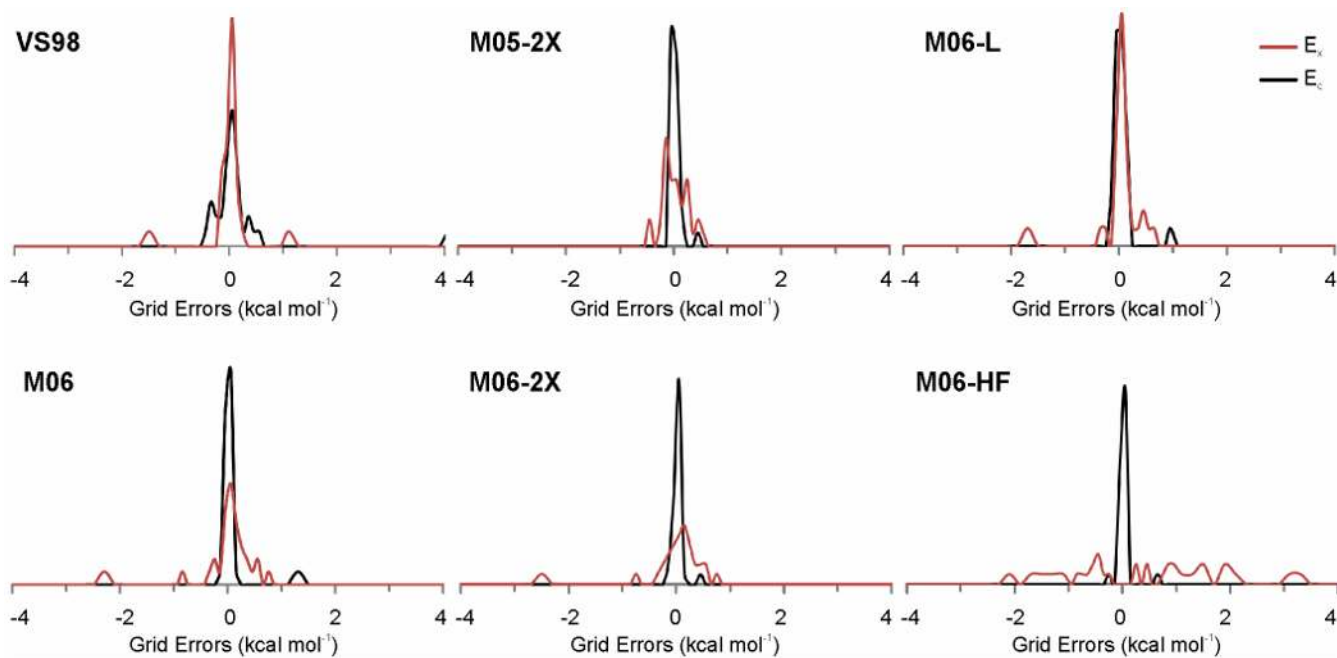
Figure 5.
Normalized distributions of grid errors (kcal mol^{-1}) for the contribution of E_x and E_c to the total energies for the reactions in Scheme 1, computed with the Q-Chem grid.
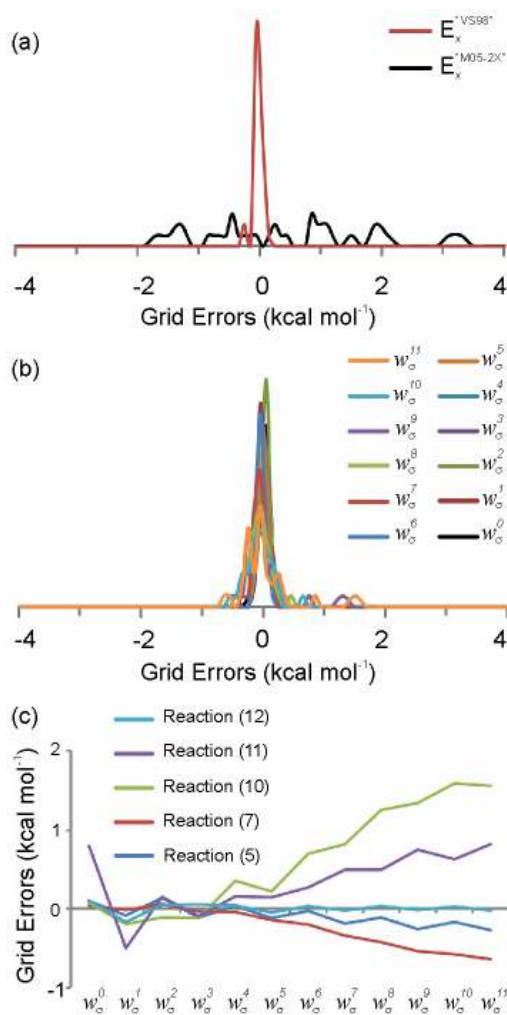
Figure 6.

(a) Normalized Q-Chem grid error distributions for the $E_x^{\text{"M05-2X"}}$ and $E_x^{\text{"VS98"}}$ components of M06-HF; (b) Q-Chem grid error distribution for each power of w_σ in

$$\sum_\sigma^{\alpha,\beta} \int d\mathbf{r} F_{X_\sigma}^{PBE}(\rho_\sigma, \nabla\rho_\sigma) w_\sigma^i$$ in the M06-HF functional (c) Q-Chem grid errors for each power of

w_σ in $\sum_\sigma^{\alpha,\beta} \int d\mathbf{r} F_{X_\sigma}^{PBE}(\rho_\sigma, \nabla\rho_\sigma) w_\sigma^i$ for representative reactions from Scheme 1.
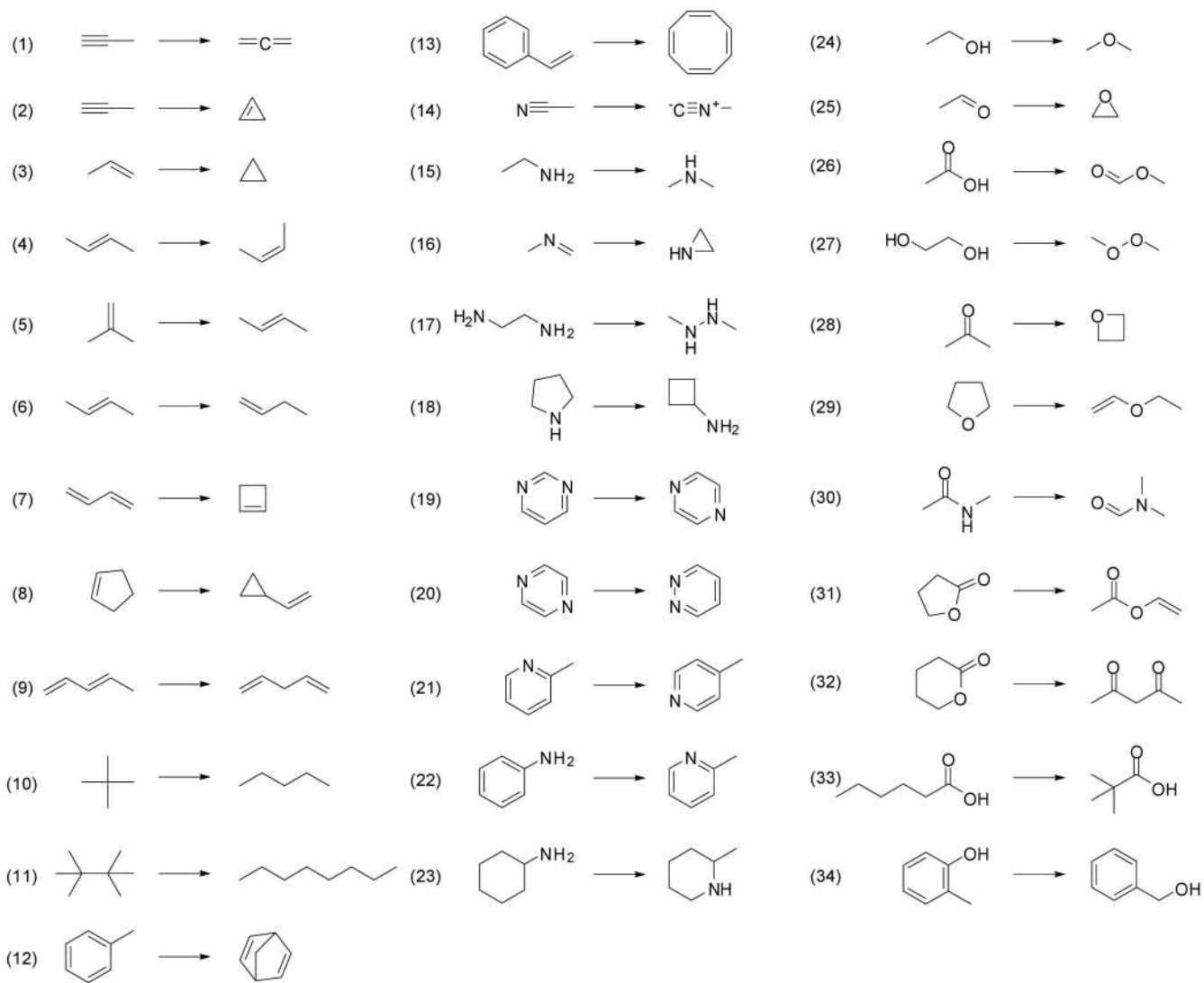
Scheme 1.

Table 1

Partitioning function, radial quadrature method, and number of radial and angular points for tested grids. All grids are pruned and utilize Lebedev's angular quadrature.[1]

	Partitioning	Radial Quadrature	Radial Points	Angular Points
Q-Chem	Becke	Euler-Maclaurin	50	194
NWChem	Erf1	Mura-Knowles	49	434
Gaussian03	SSF	Euler-Maclaurin	75	302
Fine	Erf1	Mura-Knowles	70	590
Xfine	Erf1	Mura-Knowles	100	1202

Table 2

Experimental reaction energies (ΔE, from [Ref 21]) and errors in predicted energy for the reactions in Scheme 1, relative to experiment. Mean absolute deviations (MAD), mean signed deviations (MSD), and minimum and maximum deviations (Min and Max, respectively) are also provided for each functional. The Xfine grid and TZV(2df,2pd) basis set were used. BMK, mPW2-PLYP, and B2-PLYP results are from [Ref 21]. All values are in kcal mol^{-1}.

	ΔE	B3LYP	PBE	TPSS	VS98	M05-2X	M06-L	M06	M06-2X	BMK	mPW2-PLYP	B2-PLYP
1	1.6	−3.6	−4.7	−4.5	−4.7	−2.1	−2.1	−0.6	−1.1	−2.7	−0.9	−0.9
2	21.9	1.9	−2.7	−2.4	0.2	−0.8	−3.3	−2.6	−1.7	0.8	2.5	2.5
3	7.2	1.8	−1.9	−1.5	1.4	−2.0	−4.4	−4.3	−3.4	−1.1	0.5	0.6
4	1.0	0.3	0.1	0.1	−0.7	0.2	−0.3	0.0	0.1	0.1	0.2	0.2
5	0.9	−0.6	−0.5	−0.7	1.2	0.3	−0.4	0.0	0.1	−0.2	−0.1	−0.2
6	2.6	0.6	1.0	0.7	1.2	0.0	1.4	0.9	0.3	0.3	0.2	0.3
7	11.1	4.2	−0.7	0.5	4.9	1.3	−1.5	−1.2	−0.4	−4.7	1.9	2.1
8	22.9	−3.0	−2.8	−4.0	−5.2	−2.2	−6.1	−4.9	−4.3	0.6	−1.6	−1.8
9	6.9	1.3	2.1	1.9	2.7	−0.1	2.7	1.3	0.0	0.4	0.6	0.7
10	3.6	−2.8	−2.1	−2.8	6.6	0.2	−1.5	0.3	−0.2	−1.2	−1.1	−1.2
11	1.9	−9.8	−7.2	−8.2	29.3	−0.7	−2.0	0.4	−0.8	−3.9	−4.6	−5.0
12	46.9	10.2	4.0	4.5	3.8	4.0	7.3	3.3	3.3	−0.4	6.1	6.0
13	36.0	3.2	3.1	3.9	5.3	3.9	3.9	2.1	2.0	3.4	3.7	3.7
14	24.2	−0.7	0.8	−0.9	1.5	−1.1	0.9	−1.2	−2.2	−4.1	0.3	0.6
15	7.3	0.0	0.3	−1.2	0.8	0.4	−0.1	−0.2	−0.1	0.2	0.4	0.5
16	10.8	1.6	−2.3	−1.0	1.2	−2.3	−4.6	−4.4	−3.6	−1.1	0.4	0.5
17	27.0	−1.4	−1.5	−4.1	2.7	1.0	−0.6	−0.1	−0.1	0.2	0.2	0.1
18	11.2	0.3	−0.6	0.8	−1.4	1.7	−1.2	0.0	0.7	−1.4	0.8	0.6
19	4.6	−0.5	−0.8	−0.7	−0.6	0.4	−0.6	−0.2	0.0	−0.2	−0.2	−0.3
20	20.2	−1.8	−3.1	−2.9	−2.6	−1.3	−1.9	−0.7	−0.9	0.4	−1.6	−1.9
21	0.9	0.3	0.2	0.1	0.5	0.2	0.3	0.4	0.2	0.3	0.2	0.2
22	3.2	0.4	1.2	−1.6	1.8	1.6	−0.8	0.2	0.7	−0.9	0.1	0.0
23	5.3	−0.7	−0.5	−1.9	0.3	−0.1	−0.5	−0.5	−0.6	−0.5	−0.2	−0.3
24	12.5	−1.9	−1.1	−4.3	−1.4	−1.1	−2.4	−2.0	−1.9	−2.0	−1.3	−1.3
25	26.5	1.5	−1.8	−3.6	1.9	−2.9	−2.6	−1.9	−3.7	0.4	1.1	1.1
26	18.2	−2.2	−1.4	−5.3	−1.9	−1.6	−2.1	−1.4	−2.1	−2.2	−1.7	−1.8
27	64.2	−3.5	−5.5	−11.2	−1.1	4.5	−4.3	2.3	2.0	0.8	0.0	−0.9

	ΔE	B3LYP	PBE	TPSS	VS98	M05-2X	M06-L	M06	M06-2X	BMK	mPW2-PLYP	B2-PLYP
28	31.2	2.2	−0.2	−2.2	6.6	−1.0	1.6	0.5	−1.4	−1.5	1.5	1.7
29	11.9	−3.0	−0.4	−1.2	−9.6	1.3	−1.9	−0.1	0.0	1.7	−0.5	−0.9
30	9.5	0.1	−0.5	−2.1	0.0	0.3	−0.2	−0.2	−0.3	0.1	0.1	0.0
31	14.0	−3.0	0.6	−0.8	−5.7	1.3	−0.6	0.6	0.2	2.0	−0.3	−0.7
32	7.1	−3.7	−1.5	−1.4	−10.7	2.4	−3.9	−1.4	1.2	−0.6	−1.6	−2.3
33	5.6	4.6	5.0	1.7	−4.2	2.3	2.7	2.7	2.3	2.7	3.5	3.6
34	7.3	−0.4	1.4	0.2	3.0	−0.5	2.4	1.2	0.1	0.5	−0.4	−0.4
MAD		2.3	1.9	2.5	3.7	1.4	2.2	1.3	1.2	1.3	1.2	1.3
MSD		−0.2	−0.7	−1.6	0.8	0.2	−0.8	−0.3	−0.5	−0.4	0.2	0.2
Min		−9.8	−7.2	−11.2	−10.7	−2.9	−6.1	−4.9	−4.3	−4.7	−4.6	−5.0
Max		10.2	5.0	4.5	29.3	4.5	7.3	3.3	3.3	3.4	6.1	6.0

Table 3

Analysis of grid errors for the energies of the reactions in Scheme 1 for four popular DFT integration grids. Grid errors are relative to Xfine results. All values are in kcal mol^{-1}.

	Q-Chem	NWChem	Gaussian	Fine
B3LYP				
MAD	0.08	0.00	0.01	0.00
MSD	0.04	0.00	0.00	0.00
Min	−0.17	−0.02	−0.02	−0.01
Max	0.69	0.04	0.08	0.01
PBE				
MAD	0.10	0.00	0.01	0.00
MSD	0.05	0.00	0.00	0.00
Min	−0.21	−0.02	−0.03	−0.01
Max	0.85	0.05	0.10	0.01
TPSS				
MAD	0.09	0.01	0.01	0.00
MSD	0.05	0.00	0.00	0.00
Min	−0.19	−0.03	−0.03	−0.01
Max	0.85	0.05	0.09	0.01
VS98				
MAD	0.25	0.03	0.04	0.01
MSD	0.13	0.00	0.00	0.00
Min	−0.38	−0.13	−0.22	−0.07
Max	2.80	0.21	0.37	0.05
M05-2X				
MAD	0.16	0.05	0.01	0.01
MSD	0.02	−0.02	0.01	0.00
Min	−0.39	−0.45	−0.02	−0.03
Max	0.52	0.10	0.10	0.02
M06-L				
MAD	0.20	0.05	0.02	0.01
MSD	0.09	0.03	0.00	0.00
Min	−0.84	−0.07	−0.10	−0.02
Max	0.76	0.65	0.11	0.03
M06				
MAD	0.25	0.04	0.02	0.00
MSD	0.06	0.02	0.01	0.00
Min	−1.04	−0.10	−0.08	−0.01
Max	0.75	0.31	0.12	0.02
M06-2X				
MAD	0.29	0.08	0.02	0.01
MSD	0.03	−0.02	0.00	0.00
Min	−2.02	−0.39	−0.09	−0.02

	Q-Chem	NWChem	Gaussian	Fine
Max	0.81	0.23	0.11	0.02
M06-HF				
MAD	1.20	0.20	0.03	0.02
MSD	0.05	−0.07	0.01	0.00
Min	−6.70	−1.51	−0.12	−0.05
Max	3.21	0.42	0.13	0.06

Table 4

Analysis of grid errors for the energies of the reactions in Scheme 1 for combinations of three partitioning functions (Becke, SSF, or Erf1) and two radial quadrature schemes (Euler-Maclaurin or Mura-Knowles). Results for B3LYP, PBE, and TPSS are available in SI. All grids have 50 radial points and 194 angular points. Errors are relative to Xfine results. All values are in kcal mol^{-1}.

	Euler-Maclaurin			Mura-Knowles		
	Becke	SSF	Erf1	Becke	SSF	Erf1
VS98						
MAD	0.26	0.18	0.19	0.27	0.15	0.16
MSD	0.14	0.10	0.12	0.13	0.05	0.05
Min	−0.38	−0.24	−0.27	−0.35	−0.28	−0.33
Max	2.80	1.19	1.37	3.12	0.93	0.94
M05-2X						
MAD	0.16	0.06	0.06	0.16	0.06	0.07
MSD	0.03	−0.01	−0.01	0.04	−0.01	−0.02
Min	−0.39	−0.13	−0.14	−0.32	−0.18	−0.21
Max	0.52	0.19	0.25	0.37	0.11	0.15
M06-L						
MAD	0.21	0.09	0.08	0.20	0.07	0.07
MSD	0.09	0.05	0.04	0.08	0.02	0.02
Min	−0.84	−0.13	−0.21	−0.67	−0.16	−0.17
Max	0.76	0.54	0.34	0.71	0.30	0.27
M06						
MAD	0.25	0.08	0.08	0.23	0.09	0.09
MSD	0.06	0.02	0.01	0.07	0.01	0.01
Min	−1.04	−0.17	−0.19	−0.82	−0.18	−0.16
Max	0.75	0.35	0.32	0.69	0.48	0.43
M06-2X						
MAD	0.29	0.07	0.08	0.26	0.07	0.07
MSD	0.05	0.00	0.00	0.05	−0.02	−0.02
Min	−2.02	−0.36	−0.49	−1.85	−0.20	−0.28
Max	0.81	0.30	0.33	0.66	0.14	0.17

| | Euler-Maclaurin | | | | Mura-Knowles | | | |
	Becke	SSF	Erf1		Becke	SSF	Erf1
M06-HF							
MAD	1.24	0.24	0.30		1.13	0.20	0.25
MSD	0.05	−0.04	−0.03		0.05	−0.05	−0.04
Min	−6.70	−1.35	−1.71		−6.57	−1.24	−1.61
Max	3.21	0.69	0.89		2.92	0.51	0.65

Table 5

Coefficients in the kinetic energy density enhancement factor [Eq (5)] in M05-2X[25] and the M06 suite of functionals.[10]

	M05-2X	M06-L	M06	M06-2X	M06-HF
a_0	1.0	0.3987756	0.5877943	0.46	0.1179732
a_1	−0.56833	0.2548219	−0.1371776	−0.2206052	−1.066708
a_2	−1.30057	0.3923994	0.2682367	−0.09431788	−0.1462405
a_3	5.5007	−2.103655	−2.515898	2.164494	7.481848
a_4	9.06402	−6.302147	−2.978892	−2.556466	3.776679
a_5	−32.21075	10.97615	8.710679	−14.22133	−44.36118
a_6	−23.73298	30.97273	16.88195	15.55044	−18.30962
a_7	70.22996	−23.18489	−4.489724	35.98078	100.3903
a_8	29.88614	−56.7348	−32.99983	−27.22754	38.6436
a_9	−60.25778	21.60364	−14.4905	−39.24093	−98.06018
a_{10}	−13.22205	34.21814	20.43747	15.22808	−25.57716
a_{11}	15.23694	−9.049762	12.56504	15.22227	35.90404